

Enhancing impact resistance of concrete slabs

Hemanth Kumar Anbu¹, Udhayanithi P¹,
Karthikeyan Kothandapani^{1*}, Senthilpandian M¹

¹ School of Civil Engineering, Vellore Institute of Technology, Chennai, India

* Corresponding author's e-mail: karthikeyan.kothanda@vit.ac.in

ABSTRACT

The impact resistance of concrete slabs was investigated through a comparative experimental analysis of conventional concrete (CC) and steel fiber reinforced concrete (SFRC), with a focus on dynamic performance using the ratio of crack resistance (Rcr) as a core evaluative metric. The research aims to address the limitations of CC under high-strain-rate conditions and explore the effectiveness of steel fiber reinforcement in mitigating impact-induced damage. CC slabs exhibited brittle failure with a low Rcr of 0.09, characterized by rapid crack propagation and negligible energy dissipation. In contrast, SFRC slabs demonstrated a substantial improvement in impact resistance, achieving Rcr values between 0.75 and 1.35. This performance gain is directly linked to the inclusion of 1% steel fibers, which enhanced tensile capacity, bridged developing cracks, and delayed crack propagation, ultimately shifting the failure mode from brittle to ductile. Repeated impact testing further revealed that SFRC slabs maintained structural integrity even after perforation onset. The study establishes the significance of fiber content and distribution in optimizing impact performance and reducing the risk of punching shear failure. These findings position SFRC as a structurally resilient solution for applications subjected to dynamic loading, such as protective slabs, industrial floors, and critical transportation infrastructure.

Keywords: impact loading, slab, steel fiber reinforced concrete, crack resistance.

INTRODUCTION

The construction industry faces the dual challenges of mitigating environmental impact and enhancing structural performance, necessitating innovative materials and techniques. CC, while extensively used, exhibits limitations in tensile strength, durability, and crack resistance. SFRC has emerged as a significant advancement in addressing these challenges, offering enhanced mechanical properties and durability (1–7). SFRC incorporates steel fibers into the concrete matrix, providing improved tensile strength, impact resistance, and post-cracking behavior. Its development aligns with the industry's push toward materials that meet both performance and sustainability criteria (8–12).

CC has traditionally been the material of choice for diverse structural applications due to its availability and cost-effectiveness. However,

its brittle nature under tension and susceptibility to cracking have posed limitations in dynamic and high-stress environments (13–19). In contrast, SFRC offers a significant advantage by introducing fibers that bridge cracks, distribute stresses uniformly, and enhance ductility. The frictional bond between the steel fibers and the cementitious matrix ensures resistance to crack propagation, resulting in increased toughness and energy absorption capacity. These characteristics make SFRC particularly suitable for applications requiring durability under cyclic and impact loads.

Despite these benefits, conventional concrete still dominates the market, particularly in applications where structural demands are moderate, or cost considerations take precedence. However, as the focus on sustainability and performance intensifies, SFRC is increasingly being adopted in scenarios demanding superior crack resistance, impact resilience, and long-term durability. The

integration of steel fibers enhances the load-bearing capacity of concrete and addresses deficiencies that limit the application of CC in complex and demanding environments (20–26).

The concept of advanced material designs has further widened the performance gap between SFRC and CC. Functionally graded concrete (FGC), a biomimetic-inspired material, has demonstrated the potential to optimize the performance of SFRC over CC by varying its composition across structural elements. In this context, SFRC is utilized in graded configurations to strategically enhance strength and toughness where needed while maintaining material efficiency. For example, SFRC can be concentrated in critical zones subjected to high stress, while regions with lower structural demands use conventional concrete, optimizing resource utilization and performance (27–32).

Inspiration for FGC systems arise from natural structures such as turtle shells, which exhibit a multi-layered design for impact resistance. The outer layers provide rigidity, while the inner porous core absorbs energy, a principle that can be translated into engineering applications. FGC slabs with SFRC as reinforcement layers demonstrate improved impact resistance and reduced crack propagation compared to conventional concrete. Studies reveal that these systems achieve higher failure energy thresholds and better load distribution, underscoring the superior performance of SFRC in advanced structural applications (33–42).

The integration of fibers into SFRC further amplifies its advantages over CC, particularly in reducing shrinkage-induced cracking, a common issue in cement-based materials. Conventional concrete experiences shrinkage due to moisture loss and chemical reactions, often leading to micro-cracks that compromise durability. Steel fibers mitigate this issue by resisting tensile stresses and limiting crack width, enhancing the service life of SFRC structures. This improvement in durability significantly broadens SFRC's applicability, particularly in infrastructure and high-performance buildings subjected to environmental and mechanical stresses (43–48).

In recent years, the incorporation of nanomaterials has further differentiated SFRC from conventional concrete. The addition of multi-walled carbon nanotubes (MWCNTs) to SFRC has been shown to enhance its performance by filling micro-voids, reducing porosity, and increasing

tensile strength. These properties are particularly advantageous for SFRC, as the interaction between fibers and nanotubes creates a synergistic effect, improving energy dissipation and impact resistance. In contrast, the benefits of MWCNTs are less pronounced in CC due to its lack of inherent crack-bridging capabilities, highlighting the limitations of CC in adopting advanced material innovations (49, 50).

The integration of bio-based polyurethane grout (PUG) with normal concrete (NC) has introduced a promising advancement over conventional concrete systems. By overlaying PUG mixed with quartz sand onto NC in U-shaped and beam specimens, researchers observed significant improvements in impact resistance and flexural behavior. Notably, the PUG overlay altered the brittle failure mode of NC into a more ductile response, substantially enhancing energy absorption capacity. For instance, the NC-PUGT5 specimen exhibited a sixteen-fold increase in energy absorption compared to the reference, while the NC-PUGT10 achieved impact strengths up to 68.1 times higher. Such enhancements, particularly in ductility and dynamic load tolerance, underscore the potential of PUG retrofitting in elevating concrete's resilience, capabilities that conventional concrete alone cannot achieve without external strengthening interventions (51–53).

Building upon these advancements, this study explores the development of a novel functionally graded preplaced aggregate fiber concrete (FGPAFC) system, contrasting its performance with both SFRC and CC. The FGPAFC system incorporates layers of SFRC and CC in a graded configuration, optimizing material properties to address specific structural demands. Outer layers reinforced with SFRC provide high strength and crack resistance, while inner layers using CC offer flexibility and energy absorption. This biomimetic approach draws inspiration from natural systems and represents a significant evolution from conventional material designs (54–57).

The FGPAFC system demonstrates a marked improvement in impact resistance and crack mitigation compared to CC and even traditional SFRC configurations. The integration of MWCNTs within the SFRC layers further enhances these properties by reinforcing the matrix at the nano-scale, resulting in superior toughness and durability. These innovations collectively position FGPAFC as a transformative material for

applications where both sustainability and performance are critical (58–60).

Conventional concrete, while cost-effective, cannot match the advanced mechanical and durability properties of SFRC and FGPAFC systems. The limitations of CC, particularly in high-stress or dynamic loading environments, underscore the need for enhanced materials such as SFRC. By leveraging steel fibers, functionally graded configurations, and nanotechnology, SFRC not only addresses these shortcomings but also sets new benchmarks in structural performance (61–63).

In conclusion, the evolution from conventional concrete to SFRC and advanced systems like FGPAFC highlights a paradigm shift in material science and structural engineering (64–67). SFRC, with its enhanced crack resistance and toughness, offers significant advantages over CC, while FGPAFC further expands these capabilities by integrating innovative material designs and nanotechnology. These advancements underscore the potential of SFRC and FGPAFC to redefine the future of construction, delivering sustainable and high-performance solutions for the most demanding structural applications (68–71).

EXPERIMENT WORK

Materials

The slabs were cast using M25 grade concrete, a standard choice for structural applications. The concrete exhibited an elastic modulus of 25,000 MPa, a density of 25 kN/m³, and a Poisson's ratio of 0.18, indicative of its lateral deformation behavior under compressive stress.

Reinforcement was provided using Fe 550 grade steel bars of $\phi 8$ mm diameter. The steel exhibited an elastic modulus of 200,000 MPa, a density of 7850 kN/m³, and a Poisson's ratio of 0.30, reflecting its ductile nature and ability to facilitate load redistribution under high-stress conditions.

To enhance impact resistance, 1% (by volumes) 3D steel fibers as shown in Figure 1 were incorporated into the concrete mix. This addition aimed to improve energy absorption and crack arresting capabilities, critical for high-performance slab applications under dynamic loading conditions. The specimens were developed with a deliberate focus on understanding how 3D fiber reinforcement, in conjunction with standard concrete and steel properties, could synergistically

enhance impact resistance, offering insights into designing more resilient slab systems for critical structural applications. [9, 19, 24]

Specimen preparation

This study employed a layered casting method to prepare the slab specimens. Six specimens with dimensions as listed in Table 1, were fabricated, adhering to the same concrete mix proportions and reinforcement detailing as illustrated in Figure 2.

Initially, the slab molds were thoroughly cleaned and coated with a thin layer of release oil to prevent adhesion and facilitate demolding. The casting process began by filling 50% of the mold depth with freshly mixed concrete, which was compacted using a mechanical vibrator to eliminate air pockets and ensure homogeneity. Immediately after compaction, a reinforcement mesh, was carefully positioned and securely fixed within the partially filled mold.

Subsequently, the remaining 50% of the mold depth was filled with concrete, and additional compaction was applied to achieve a well-bonded and integrated structure. This layered casting method ensured optimal bond strength between the layers and minimized the likelihood of weak planes forming within the slabs.

To get a smooth, consistent texture, the example's surfaces were leveled and smoothed with a trowel after casting. In order to give the concrete time to set, the molds were left in place for a whole day. The slabs were meticulously demolded and exposed to water curing for 28 days after the initial setting time, guaranteeing the development of the required strength and durability qualities.

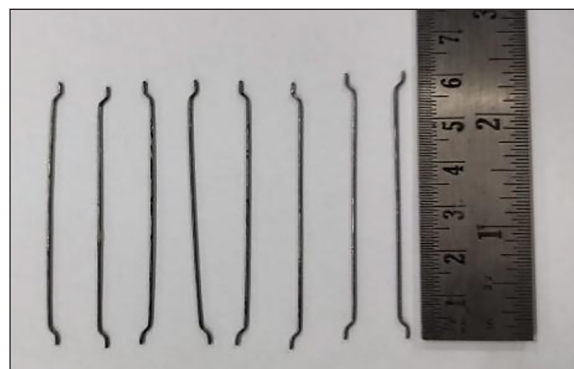


Figure 1. Layer setups

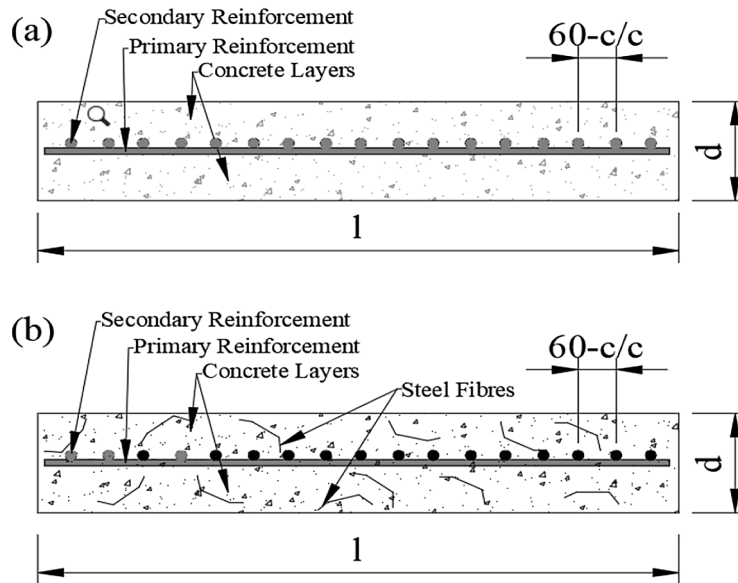


Figure 2. Layer setups: (a) Conventional concrete (CC) and (b) Steel fiber reinforced concrete (SFRC)

The preparation process was systematically executed to maintain consistency across all specimens, enabling reliable and repeatable results during subsequent testing.

Experimental setup

Standardized testing protocols were used to assess the slab specimens' compressive and impact strengths in the experimental setup. Using three replicates for each mixture to obtain an average result, 100 mm cubic specimens were tested for compressive strength in compliance with IS 516. According to ACI Committee 544-2R, impact resistance was evaluated using the drop-weight impact test, which used a straightforward device that could release a 2.25 kg object onto the slab surface from a height of 0.457 m, as seen in Figure 3. Failure was determined by the apparent spread of cracks from the slab's top to bottom surface, and the number of hits needed to cause first cracking (FC1) and total failure (FC2) were noted. Equation 1 was utilized to get the impact energy (U) given per hit. Impact parameters, including drop height, hammer mass, and loading configuration,

were systematically designed to simulate realistic accidental impacts such as falling objects or debris strikes. By adopting dynamic tests such as drop-weight impacts, the study aimed to replicate high strain-rate conditions where fiber reinforcement mechanisms become most effective. The controlled impact energy levels allowed the researchers to differentiate performance based on fiber action, slab stiffness, and overall toughness.

$$U = m \times g \times h \times N \quad (1)$$

where: m is the drop mass (2.25 kg), g is the acceleration due to gravity (9.81 m/s^2), h is the drop height (0.457 m), and N is the number of hits. Each impact was treated as delivering a uniform amount of energy, enabling precise quantification of the slab's impact resistance. This experimental setup ensured reliable and repeatable results for assessing the structural performance of the specimens.

RESULTS

Impact results

The impact resistance test results for SFRC slabs and CC slabs demonstrate how important steel fibers are to improving the material's performance under dynamic loading circumstances. With matching impact energies of $70.61 \text{ N}\cdot\text{m}$ and $171.48 \text{ N}\cdot\text{m}$, respectively, the CC showed initial

Table 1. Specimen dimensions

Length (l) (mm)	Width (b) (mm)	Depth (d, thk.) (mm)
500	500	100
750	500	100
1000	500	100

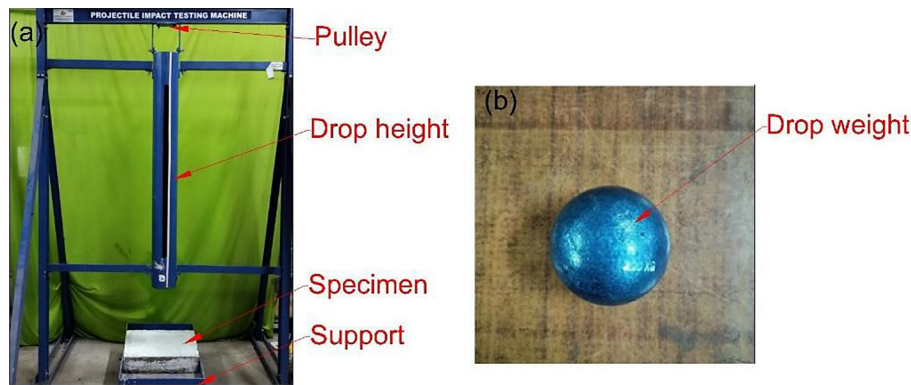


Figure 3. Test setup

cracking (IC) and failure (FC) at impacts 7 and 17 for the 500×500 mm slabs. The SFRC slab, on the other hand, demonstrated notable improvement, with failure delaying until 51 impacts, resulting in an energy of $514.44 \text{ N}\cdot\text{m}$, a nearly 200% increase in failure energy, and cracking after 4 impacts (impact energy: $40.35 \text{ N}\cdot\text{m}$). Steel fibers, which efficiently bridge microcracks and postpone their progression into macrocracks by transferring tensile loads across crack sides, are responsible for this increased resistance. Because of its high tensile strength and ductility, the fiber reduces the rate at which cracks spread by mitigating stress accumulation at critical spots.

For the 500×750 mm slabs, while cracking occurred after 4 impacts for both CC and SFRC, producing identical cracking energies of $40.35 \text{ N}\cdot\text{m}$, a significant divergence was observed at failure. The SFRC slab resisted 47 impacts, achieving a failure energy of $474.10 \text{ N}\cdot\text{m}$, compared to 42 impacts and $423.66 \text{ N}\cdot\text{m}$ for CC. This difference is primarily due to the post-cracking tensile load-carrying capacity of the steel fibers, which limit crack widening by redistributing the tensile stresses. As the SFRC slabs absorbed additional impacts, the fibers sustained higher loads without rupture, enhancing the slab's energy absorption capacity.

The 500×1000 mm slabs demonstrated similar trends, with SFRC outperforming CC significantly. Cracking occurred after 10 impacts (impact energy: $100.87 \text{ N}\cdot\text{m}$) for CC, compared to 15 impacts (impact energy: $151.31 \text{ N}\cdot\text{m}$) for SFRC. At failure, the SFRC slab resisted 50 impacts with a failure energy of $504.36 \text{ N}\cdot\text{m}$, doubling the performance of the CC slab, which failed after 25 impacts and an energy of $252.18 \text{ N}\cdot\text{m}$. The larger slab size increases the area over which tensile stresses are distributed, reducing localized

stresses. However, for CC slabs, this stress redistribution is insufficient to prevent rapid crack propagation. In contrast, SFRC slabs benefit from the anchoring effect of fibers, which dissipate impact energy by transferring stresses along their lengths and engaging the surrounding concrete matrix. The superior energy absorption in SFRC slabs arises from the fiber's ability to delay crack coalescence, prolonging the pre-failure stage and allowing for greater energy dissipation through micro-crack bridging.

The increased cracking and failure energies in SFRC slabs are further influenced by the dynamic interaction between compressive and tensile stress waves during impact loading. Upon each impact, localized compressive stresses at the slab's point of contact generate tensile stress waves that radiate outward, leading to crack initiation and propagation. In CC slabs, these stress waves rapidly exceed the concrete's tensile strength, causing brittle failure. Conversely, in SFRC, steel fibers interrupt and redistribute these stress waves, reducing their intensity and preventing rapid crack growth. Additionally, the pullout resistance of steel fibers during crack widening contributes to the slab's ability to sustain additional impacts, highlighting the ductile failure mechanism of SFRC compared to the brittle failure of CC. This ductility, combined with the inherent toughness provided by the steel fibers, underscores the superior performance of SFRC in resisting impact loads (Table 2).

Impact ductility and post-cracking energy

A more thorough insight of the structural performance under dynamic loads is offered by the impact ductility (ID) and extra post-cracking energy (PE) parameters. Because of its poor capacity to absorb energy in the plastic range, CC slab's

Table 2. Impact count

Dimension (mm)	CC		SFRC	
	IC	FC	IC	FC
500 × 500	7	17	4	51
500 × 750	4	42	4	47
500 × 1000	10	25	15	50

Note: IC and FC are initial and final crack count respectively.

ID was consistently lower than that of SFRC. The SFRC 500 × 500 mm slabs, for instance, attained an ID of over 2.9, which is far higher than the CC slabs' ID of 1.0. This improvement, which ranges from 170% to 200%, demonstrates the increased ductility that steel fibers provide. The remarkable energy retention capabilities of SFRC are further demonstrated by the increased PE values. In the 500 × 1000 mm specimens, for example, SFRC slabs showed an PE of roughly 353 N·m, which was more than 130% higher than the CC slab's PE of only 151 N·m.

The mechanical characteristics of steel fibers are principally responsible for the noted improvement in both ID and PE. The fibers serve as crack bridges, regulating the crack width and dispersing tensile stresses throughout the crack plane when cracks form under impact loading. By postponing the spread of cracks and permitting the slab to undergo plastic deformation while still dissipating energy, this crack-bridging process avoids abrupt failure. Additionally, the fibers' high tensile strength and anchorage bond with the concrete matrix ensure that they remain engaged under loading, further contributing to energy absorption. The enhanced ductility and post-cracking energy capacity of SFRC can be technically explained by the synergistic interaction between the fibers and the surrounding concrete, which transforms a brittle failure mode into a more ductile, energy-dissipative behavior. This performance is particularly beneficial in applications where resistance to high-energy impacts and delayed catastrophic failure are critical (Table 3).

Effect of steel fibres on impact energy

The integration of steel fibres in concrete slabs significantly enhances their impact resistance, as evident from the comparative analysis of CC and SFRC slabs. The variation in the number of impacts and corresponding impact energy reveals the critical role of fibre reinforcement in

improving both cracking and failure characteristics under dynamic loading.

Number of impacts

The data indicates a marked improvement in the impact resistance of SFRC slabs compared to CC. For instance, the 500 × 500 mm slab recorded 7 IC and 17 FC in CC, whereas the SFRC counterpart required only 4 impacts to IC but sustained up to 51 impacts to FC. This dramatic increase in failure resistance underscores the enhanced post-cracking ductility provided by steel fibres. Similarly, for the 500 × 750 mm slab, the number of impacts to FC rose from 42 in CC to 47 in SFRC, despite both materials requiring the same number of impacts to reach IC. The 500 × 1000 mm slab demonstrated a significant improvement as well, with impacts to IC increasing from 10 to 15 and impacts to FC rising from 25 in CC to 50 in SFRC.

The occurrence of this behavior is attributed to the role of steel fibres in mitigating crack propagation. Upon impact, stress concentration at micro-cracks in Conventional Concrete leads to rapid crack widening, causing premature failure. In SFRC, the steel fibres act as bridging elements across cracks, redistributing stress and preventing localized crack growth. This bridging mechanism delays failure and allows the structure to absorb more energy before collapse.

Impact energy

The influence of steel fibres on impact energy was equally pronounced. For the 500 × 500 mm slab, the impact energy at IC decreased from 70.61 J in CC to 40.35 J in SFRC, while the energy at FC surged from 171.48 J in CC to 514.44 J in SFRC. This significant increase in failure energy highlights the fibres' ability to redistribute stresses effectively and delay catastrophic failure. In the case of the 500 × 750 mm slab, the impact energy at IC remained constant at 40.35 J for both materials, but the energy at FC increased from

Table 3. Impact energy

Dimension (mm)	CC		SFRC	
	IC (N-mm)	FC (N-mm)	IC (N-mm)	FC (N-mm)
500 × 500	70.61	171.48	40.35	514.44
500 × 750	40.35	423.66	40.35	474.10
500 × 1000	100.87	252.18	151.31	504.36

Note: IC and FC are initial and final crack count respectively.

423.66 J in CC to 474.10 J in SFRC, reflecting the fibres’ contribution to post-cracking resilience. The 500 × 1000 mm slab exhibited an even more substantial improvement, with IC energy increasing from 100.87 J in CC to 151.31 J in SFRC and FC energy rising from 252.18 J to 504.36 J.

This behavior can be explained by the ability of steel fibres to improve energy dissipation under dynamic loading. During impact, fibres embedded in the concrete matrix transfer tensile stresses across cracks, enhancing the material’s capacity to resist further fracturing. The lower IC energy in SFRC slabs suggests that the fibres allow for micro-cracking to occur at lower energy levels, creating a distributed damage pattern that prevents brittle failure. At FC, the fibres continue to provide resistance by anchoring the cracked segments, which significantly increases the energy required for complete structural disintegration.

Interpretation and Implications

The analysis reveals a consistent trend, while the presence of steel fibres slightly reduces the energy required for cracking, it significantly boosts the energy required for failure. The fibres enhance the tensile capacity and toughness of the concrete, effectively transforming the material behavior from brittle to ductile. Additionally, the effectiveness of the fibres increases with slab size, as larger elements provide more surface area for fibre stress transfer, resulting in improved impact resistance.

The impact resistance of concrete slabs can be significantly increased by adding steel fibers, especially during the failure stage. This paves the path for safer and more resilient infrastructure designs by highlighting the significance of SFRC adoption in structural applications that demand strong energy absorption and post-cracking performance.

Ratio of crack resistance of the slab

The ratio of fracture resistance (Rcr), a non-dimensional metric, was developed to measure

how well slabs performed in withstanding impacts during the service and ultimate phases. The following formula was used to determine the parameter:

$$Rcr = \frac{U2}{Compressive\ strength} \quad (2)$$

where: *U2* stands for the energy that the slab ultimately absorbs. Figures 4 and 5 show the computed Rcr values for each tested slab, demonstrating the notable variations in the slab types’ performance in terms of fracture resistance.

In comparison to its compressive strength, the conventional concrete (CC) slab’s Rcr value ranged from 6.96 to 17.2, indicating a lesser level of crack resistance in the end. Its brittle character is supported by this behavior, as the slab collapses abruptly under impact loading with little energy absorption. On the other hand, because of the steel fibers’ improved ductility and energy dissipation, the steel fiber reinforced concrete (SFRC) slabs showed higher Rcr values, ranging from 19.25 to 20.48. Table 4 shows the crack resistance ratio for the tested specimens.

The SFRC slabs in the upper layers exhibited Rcr values greater than 19, indicating superior resistance to repeated impacts compared to their compressive strength. For instance, the SFRC slab achieved an Rcr value of 20.89, signifying its ability to sustain repeated impacts while delaying crack propagation and ultimate failure. This improvement is attributed to the bridging action of steel fibers, which effectively resisted crack initiation and reduced crack growth under dynamic loading.

The results emphasize the importance of Rcr as a reliable metric for evaluating the impact resistance of concrete slabs. The bridging action of steel fibers played a pivotal role in improving the Rcr values by delaying crack initiation and controlling crack propagation.

Furthermore, the findings underscore the potential of SFRC slabs to offer higher durability

Table 4. Ratio of crack resistance

Dimension (mm)	CC	SFRC
500 × 500	6.96	20.89
500 × 750	17.20	19.25
500 × 1000	10.24	20.48

and energy dissipation under dynamic loading conditions, making them suitable for applications requiring enhanced resistance to impact forces.

MODE OF FAILURE

Brittle failure of conventional concrete slab

The CC slab demonstrated a brittle failure mechanism when subjected to repeated impacts. The slab developed multiple fractures due to the complete loss of its structural integrity. This failure was primarily caused by the inability of the material to absorb and dissipate the impact energy effectively. The absence of fibers in the CC slab contributed to its rapid degradation under impact, leading to the fragmentation of the concrete into four distinct sections. The loss of cohesion between the cement matrix and aggregates during the impact sequence led to significant geometric alterations of the slab, which ultimately compromised its load-bearing capacity. This brittle behavior is consistent with the typical response of unreinforced concrete, where cracks propagate rapidly, causing catastrophic failure under dynamic loading conditions.

Ductile failure of steel fiber reinforced concrete slab

In contrast to the CC slab, the SFRC slab exhibited a ductile failure mechanism. Following the initial crack formation, the slab with fibers endured successive impacts and absorbed additional energy. The impact-induced cracks in the SFRC slab did not result in immediate fragmentation; instead, they spread across the slab's surface, forming multiple macro-cracks. This distribution of cracks allowed the slab to maintain a greater surface area under tension, which significantly delayed the failure process. The enhanced energy absorption capability of the SFRC slab was attributed to the fiber bridging action, which effectively mitigated the development of large, catastrophic cracks. This behavior aligns with the

findings of previous research, where the addition of fibers was shown to increase the slab's overall impact resistance and ductility. Moreover, the fibers contributed to the formation of smaller, more distributed cracks, thereby preventing abrupt, brittle failures.

Perforation failure in fiber-reinforced slabs

The SFRC Slabs, particularly those with higher fiber content, experienced a failure mode characterized by both compressive cracking and perforation. These slabs initially exhibited signs of compressive cracking under low-velocity impacts. However, after repeated impacts, a more significant failure mechanism emerged, wherein the steel ball penetrated the slab, causing a perforation failure. Unlike the CC slab, the SFRC slabs retained a degree of structural integrity due to the fibers, which helped hold the slab together even after substantial material dislodgement. The fibers acted as a reinforcement, preventing the complete collapse of the slab despite the formation of perforations.

The perforation was not evident at the early stages of impact but became apparent as the repeated blows from the steel ball propagated cracks through the slab. The first shear damage initiated micro-cracking within the slab's matrix, which gradually expanded towards the outer edges, eventually leading to a perforation. However, the addition of fibers in the upper and lower layers of SFRC slabs significantly delayed the onset of perforation, primarily by enhancing crack bridging capabilities. The fibers mitigated crack propagation, thus postponing complete failure.

Impact ductility and crack bridging effect in SFRC slabs

It is notable that the SFRC slab's impact ductility has significantly improved. Even when fissures started to spread, the slab's increased fiber content kept them structurally sound. In order to keep the fiber network continuous throughout the widening fissures, the fibers were essential in bridging the gaps. As a result, the failure mode changed from catastrophic cracking to perforation and the fracture spread was greatly limited. The slabs could withstand significant tensile stresses even in the presence of cracks thanks to this increase in impact ductility, providing a higher degree of performance under impact loading.

When fiber bridging and energy dissipation work together, this hole failure mode shows how much more impact resistant SFRC slabs are than regular concrete. These slabs' structural resilience is greatly increased by the fibers' capacity to stop cracks from spreading and absorb impact energy, which qualifies them for uses where resistance to impact and dynamic loads is essential.

These findings confirm the previously reported behavior of fiber-reinforced concrete under impact loading, where the fiber reinforcement not only improved the initial crack resistance but also played a pivotal role in transforming potential brittle failure into more controlled perforation.

Failure mechanism

Shearing, compaction, and cracking of the concrete material under dynamic stresses are the main mechanisms that cause failure. The acting forces – tension, compression, or lateral restraint – that control the failure's course and intensity have a major impact on these failure modes. The ultimate fracture patterns and overall slab failure, however, are mostly determined by the concrete's inherent characteristics and the degree of fiber insertion.

Localized failure mechanisms

Under impact loading, the initial failure is often localized to the point of contact between the impactor and the slab. This localized damage includes surface cracking, material spalling, and compaction at the impact site. The transfer of impact energy into the concrete matrix results in compressive bending failure, where the material undergoes significant deformation along the

impact plane. As the force propagates through the slab, shear stress and strain in the transverse direction led to internal debonding between the fibers and the matrix. This debonding weakens the structural integrity and promotes the spread of cracks. Additionally, tensile bending in the tension zone amplifies the fiber detachment from the matrix, allowing cracks to progress to subsequent layers, further compromising the slab's ability to resist impact loads.

Failure progression in fiber-reinforced slabs

In fiber-reinforced slabs, the progression of failure mechanisms differs due to the enhanced crack-bridging capability of the fibers. During the impact, fiber rupture and matrix failure are the primary modes of failure observed. While the cracks originate at the point of impact, the inclusion of fibers significantly delays their propagation. The early transfer of kinetic energy to the fibers illustrates their ability to mitigate damage by linking cracks and redistributing stresses to adjacent regions of the concrete. Despite this advantage, a critical challenge arises from the separation of fibers from their matrix. This fiber-matrix debonding reduces the structural integrity of the slab and impairs its strength properties over time, making detection during service a significant issue.

Punching shear and crack formation

In slabs subjected to high-impact loads, punching shear failure becomes a prominent failure mode, particularly in the impact contact area. The presence of fiber content in both the compression and tension zones reduces the formation of large cracks. Instead, the slab exhibits

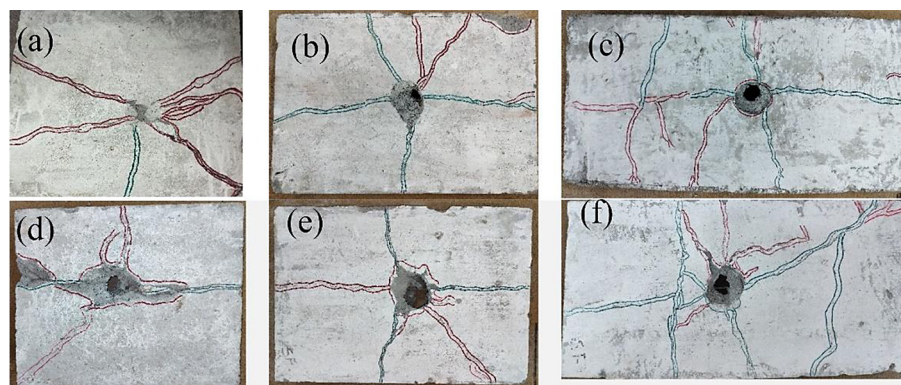


Figure 4. Front face of slab: (a), (b) and (c) shows CC slabs, (d), (e) and (f) shows SFRC slabs (Green indicates initial crack and Red indicates final cracks)

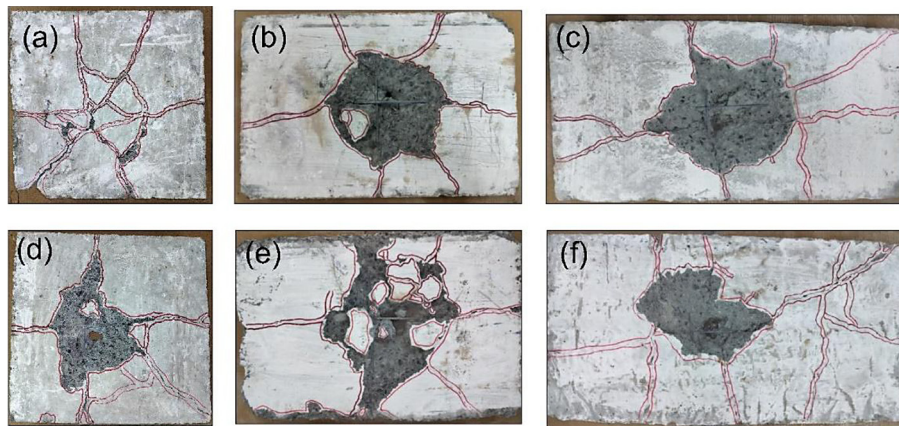


Figure 5. Back face of slab: (a), (b) and (c) shows CC slabs, (d), (e) and (f) shows SFRC slabs

a combination of localized crushing and micro-crack networks, which delays catastrophic failure. This is consistent with prior studies that emphasize the role of fibers in controlling crack propagation and enhancing the slab's resistance to impact. The bridging action of fibers reduces the likelihood of major crack formation by effectively transferring stresses across the crack plane, thereby maintaining the slab's integrity for a longer duration.

Influence of material composition on failure modes

The observed modes of failure are inherently dependent on the material composition of the slab. CC slabs tend to fail through brittle fracture mechanisms, with rapid crack propagation leading to complete disintegration. In contrast, SFRC slabs exhibit more ductile failure behavior, where the fibers contribute to energy absorption and retardation of crack growth. The extent of fiber bridging action plays a pivotal role in determining the slab's ability to withstand successive impacts. Fiber content not only reduces the extent of damage but also transforms the failure mode from brittle to ductile, thereby enhancing the overall impact resistance.

These modes of failure, encompassing localized damage, fiber-matrix interaction, and punching shear, provide valuable insights into the dynamic behavior of slabs under impact loading. The findings underscore the significance of material composition and fiber integration in mitigating the detrimental effects of high-velocity impacts, ultimately improving the performance and durability of concrete slabs in structural applications.

CONCLUSIONS

1. The brittle failure of CC slabs was typified by an abrupt collapse because of the concrete's poor energy-dissipation capabilities. Fragmentation resulted from the CC slab's lack of fibers, which made it unable to endure repeated impacts. This kind of behavior is common in unreinforced concrete, as cracks spread swiftly under dynamic loads until the structure fails completely. Conversely, SFRC slabs showed a mode of ductile failure. Steel fibers allowed the slab to absorb more energy by bridging the crack surfaces, which greatly postponed the creation of catastrophic cracks. By distributing stresses over a greater surface and withstanding tensile forces, the fibers helped postpone final failure, enabling the slab to sustain several strikes.
2. SFRC slabs, especially those with fiber content, demonstrated a perforation failure mode after multiple impacts. Initially, these slabs exhibited compressive cracking, but with repeated impacts, the steel ball penetrated the slab. Despite significant material dislodgement, the fibers held the slab together, preventing total collapse. This failure mode, observed as crack propagation followed by perforation, shows how fibers can mitigate crack growth and delay the onset of perforation. Fiber reinforcement delays the crack propagation by enhancing crack bridging, which absorbs and redistributes energy, preventing the slab from failing suddenly.
3. The fiber bridging effect is pivotal in enhancing the impact resistance of SFRC slabs. Fibers effectively link the cracks, preventing

rapid propagation by redistributing the internal stresses. This leads to a more uniform crack pattern rather than the formation of a single large crack, which would cause catastrophic failure. In fiber-reinforced slabs, the initial cracking at the point of impact is delayed due to the transfer of energy to the fibers, which then absorb the impact load. This process helps to slow down the crack growth and contributes to the overall structural stability of the slab under dynamic loading conditions.

4. SFRC results in greater ductility and improved tensile strength, which are crucial for enhancing the impact resistance of the slab. SFRC slabs with higher fiber content exhibited R_{cr} values greater than 19, indicating superior resistance to repeated impacts compared to their compressive strength. This is because the fibers provide additional tensile strength to the concrete, which is typically weak in tension. When cracks form, the fibers bridge the cracks, redistributing the applied load across a larger area, thereby reducing the likelihood of catastrophic failure and improving the overall energy dissipation capacity.
5. In slabs subjected to high-impact loads, punching shear failure occurs at the point of contact with the impactor, leading to localized material crushing. However, SFRC slabs demonstrated reduced punching shear failure due to the reinforcing effect of fibers. The fibers distributed the impact force across the slab and minimized the formation of large cracks. Instead, the slab exhibited micro-crack networks, which allowed it to resist high localized stresses. The fibers' ability to bridge cracks and transfer stresses through the slab reduces the likelihood of major crack formation, thus enhancing the slab's impact resistance.
6. The improved impact resistance of SFRC slabs, demonstrated through higher R_{cr} values and ductile failure modes, shows their suitability for applications where resistance to impact and dynamic loads is critical. The steel fibers effectively dissipate the energy from repeated impacts, delaying crack initiation and controlling crack propagation. This makes SFRC slabs particularly beneficial in environments subject to heavy traffic or other dynamic loads, where concrete elements need to withstand repeated impacts without significant degradation.

7. Future research should focus on optimizing the fiber geometry, dosage, and distribution within the matrix. Additionally, exploring hybrid reinforcement strategies combining different types of fibers or incorporating other materials such as polymers could further enhance the impact resistance and overall durability of SFRC slabs. By fine-tuning these parameters, it is possible to create concrete elements that offer superior performance under dynamic loading, ensuring structural resilience and longevity in impact-prone environments.

Acknowledgement

The authors thank VIT for providing “VIT RGEMS SEED GRANT” for carrying out this research work.

REFERENCES

1. Li Y., Shen J., Lin H., Li Y. Optimization design for alkali-activated slag-fly ash geopolymer concrete based on artificial intelligence considering compressive strength, cost, and carbon emission, *J. Build. Eng.* 2023; 75. <https://doi.org/10.1016/j.jobe.2023.106929>
2. Zhang S., Li Z., Ghiassi B., Yin S., Ye G. Fracture properties and microstructure formation of hardened alkali-activated slag/fly ash pastes, *Cement Concr. Res.* 2021; 144. <https://doi.org/10.1016/j.cemconres.2021.106447>
3. Shilar F.A., Ganachari S.V., Patil V.B., Nisar K.S. Evaluation of structural performances of metakaolin based geopolymer concrete, *J. Mater. Res. Technol.* 2022. <https://doi.org/10.1016/j.jmrt.2022.08.020>
4. A. Bouaissi, Li L. yuan, M.M. Al Bakri Abdullah, Q.B. Bui, Mechanical properties and microstructure analysis of FA-GGBS-HMNS based geopolymer concrete, *Construct. Build. Mater.* 2019; 210: 198–209. <https://doi.org/10.1016/j.conbuildmat.2019.03.202>
5. WBCSD. World Business Council for Sustainable Development and International Energy Agency Cement Technology Roadmap 2009: Carbon Emissions Reductions up to 2050, World Business Council for Sustainable Development IEA (International Energy Agency), 2009.
6. Eisa M.S., Basiouny M.E., Fahmy E.A. Drying shrinkage and thermal expansion of metakaolin-based geopolymer concrete pavement reinforced with biaxial geogrid, *Case Stud. Constr. Mater.* 2022; 17. <https://doi.org/10.1016/j.cscm.2022.e01415>

7. Yu M., Lin H., Wang T., Shi F., Li D., Chi Y., et al. Experimental and numerical investigation on thermal properties of alkali-activated concrete at elevated temperatures, *J. Build. Eng.* 2023; 74. <https://doi.org/10.1016/j.jobe.2023.106924>
8. Oesterlee C. Structural analysis of a composite bridge girder combining UHPFRC and reinforced concrete. *High Performance Concrete*, 2008; 1–8.
9. Murali G., Santhi A.S., Ganesh G.M. Impact resistance and strength reliability of fiber-reinforced concrete in bending under drop weight impact load, *International Journal of Technology* 2014; 5. <https://doi.org/10.14716/ijtech.v5i2.403>
10. Murali G., Abid S.R., Abdelgader H.S., Amran Y.H.M., Shekarchi M., Wilde K. Repeated projectile impact tests on multi-layered fibrous cementitious composites, *Int. J. Civ. Eng.* 2021. <https://doi.org/10.1007/s40999-020-00595-4>
11. Prasad N., Murali G. Exploring the impact performance of functionally-graded preplaced aggregate concrete incorporating steel and polypropylene fibres, *J. Build. Eng.* 2021; 35. <https://doi.org/10.1016/j.jobe.2020.102077>
12. Prasad N., Murali G., Abid S.R., Vatin N., Fediuk R., Amran M. Effect of needle type, number of layers on FPAFC composite against low-velocity projectile impact, *Buildings* 2021; 11. <https://doi.org/10.3390/buildings11120668>
13. Moghadam A.S., Omidinasab F., Dalvand A. Experimental investigation of (FRSC) cementitious composite functionally graded slabs under projectile and drop weight impacts, *Construct. Build. Mater.* 2020; 237: 117522. <https://doi.org/10.1016/j.conbuildmat.2019.117522>
14. Quek S.T., Lin V.W.J., Maalej M. Development of functionally-graded cementitious panel against high-velocity small projectile impact, *Int. J. Impact Eng.* 2010; 37: 928–941. <https://doi.org/10.1016/j.ijimpeng.2010.02.002>
15. Mastali M., Ghasemi Naghibdehi M., Naghipour M., Rabiee S.M. Experimental assessment of functionally graded reinforced concrete (FGRC) slabs under drop weight and projectile impacts, *Construct. Build. Mater.* 2015; 95: 296–311. <https://doi.org/10.1016/j.conbuildmat.2015.07.153>
16. Li P.P., Sluijsmans M.J.C., Brouwers H.J.H., Yu Q.L. Functionally graded ultra-high performance cementitious composite with enhanced impact properties, *Compos. B Eng.* 2020; 183. <https://doi.org/10.1016/j.compositesb.2019.107680>
17. Rhee H., Horstemeyer M.F., Hwang Y., Lim H., El Kadiri H., Trim W. A study on the structure and mechanical behavior of the Terrapene Carolina carapace: a pathway to design bio-inspired synthetic composites, *Mater. Sci. Eng. C* 2009; 29: 2333–2339. <https://doi.org/10.1016/j.msec.2009.06.002>
18. Ong C.W.R., Zhang M.H., Du H., Pang S.D. Functionally layered cement composites against projectile impact, *Int. J. Impact Eng.* 2019; 133: 103338. <https://doi.org/10.1016/j.ijimpeng.2019.103338>
19. Prasad N., Murali G. Research on flexure and impact performance of functionally-graded two-stage fibrous concrete beams of different sizes, *Construct. Build. Mater.* 2021; 288: 123138. <https://doi.org/10.1016/j.conbuildmat.2021.123138>
20. Murali G., Abid S.R., Al-Lami K., Vatin N.I., Dixit S., Fediuk R. Pure and mixed-mode (I/III) fracture toughness of preplaced aggregate fibrous concrete and slurry infiltrated fibre concrete and hybrid combination comprising nano carbon tubes, *Construct. Build. Mater.* 2023; 362. <https://doi.org/10.1016/j.conbuildmat.2022.129696>
21. Murali G., Abid S.R., Vatin N.I., Amran M., Fediuk R. Influence of height and weight of drop hammer on impact strength and fracture toughness of two-stage fibrous concrete comprising nano carbon tubes, *Construct. Build. Mater.* 2022; 349. <https://doi.org/10.1016/j.conbuildmat.2022.128782>
22. Karthik S., Raja Mohan K.S., Murali G. Investigations on the response of novel layered geopolymer fibrous concrete to drop weight impact, *Buildings* 2022; 12. <https://doi.org/10.3390/buildings12020100>
23. Murali G., Abid S.R., Amran M., Fediuk R., Vatin N., Karelina M. Combined effect of multi-walled carbon nanotubes, steel fibre and glass fibre mesh on novel two-stage expanded clay aggregate concrete against impact loading, *Crystals* 2021; 11. <https://doi.org/10.3390/cryst11070720>
24. Murali G., Abid S.R., Karthikeyan K., Haridharan M.K., Amran M., Siva A. Low-velocity impact response of novel prepacked expanded clay aggregate fibrous concrete produced with carbon nano tube, glass fiber mesh and steel fiber, *Construct. Build. Mater.* 2021; 284. <https://doi.org/10.1016/j.conbuildmat.2021.122749>
25. Elakhras A.A., Seleem M.H., Sallam H.E.M. Intrinsic fracture toughness of fiber reinforced and functionally graded concretes: an innovative approach, *Eng. Fract. Mech.* 2021; 258. <https://doi.org/10.1016/j.engfracmech.2021.108098>
26. Lai J., Yang H., Wang H., Zheng X., Wang Q. Penetration experiments and simulation of three-layer functionally graded cementitious composite subjected to multiple projectile impacts, *Construct. Build. Mater.* 2019; 196: 499–511. <https://doi.org/10.1016/j.conbuildmat.2018.11.154>
27. Zhang P., Su J., Guo J., Hu S. Influence of carbon nanotube on properties of concrete: a review, *Construct. Build. Mater.* 2023; 369. <https://doi.org/10.1016/j.conbuildmat.2023.130388>
28. Lu D., Shi X., Zhong J. Nano-engineering the

- interfacial transition zone in cement composites with graphene oxide, *Construct. Build. Mater.* 2022; 356. <https://doi.org/10.1016/j.conbuildmat.2022.129284>
29. Sanchez F., Sobolev K. Nanotechnology in concrete - a review, *Construct. Build. Mater.* 2010. <https://doi.org/10.1016/j.conbuildmat.2010.03.014>
30. Han B., Yu X., Kwon E. A self-sensing carbon nanotube/cement composite for traffic monitoring, *Nanotechnology* 2009; 20. <https://doi.org/10.1088/0957-4484/20/44/445501>
31. Li Y., Li H., Wang Z., Jin C. Effect and mechanism analysis of functionalized multi-walled carbon nanotubes (MWCNTs) on C-S-H gel, *Cement Concr. Res.* 2020; 128. <https://doi.org/10.1016/j.cemconres.2019.105955>
32. Nam I.W., Park S.M., Lee H.K., Zheng L. Mechanical properties and piezoresistive sensing capabilities of FRP composites incorporating CNT fibers, *Compos. Struct.* 2017; 178: 1–8. <https://doi.org/10.1016/j.compstruct.2017.07.008>
33. Korayem A.H., Tourani N., Zakertabrizi M., Sabziparvar A.M., Duan W.H. A review of dispersion of nanoparticles in cementitious matrices: nanoparticle geometry perspective, *Construct. Build. Mater.* 2017; 153: 346–357. <https://doi.org/10.1016/j.conbuildmat.2017.06.164>
34. Bureau of Indian Standards (Bis). Code of Practice – Specification for Coarse and Fine Aggregate from Natural Sources for Concrete: New Delhi: BIS; 1970. Standard No IS 383: 2002., n.d.
35. Astm, C939-10. Standard Test Method for Flow of Grout for Preplaced-Aggregate Concrete (Flow Cone Method), 2010; 4: 9–11. ASTM International, <https://doi.org/10.1520/C0939-16A>
36. Luo J.L. Fabrication and Functional Properties of Multi-Walled Carbon Nanotube/cement Composites, 2009.
37. Parveen S., Rana S., Fanguero R., Paiva M.C. Microstructure and mechanical properties of carbon nanotube reinforced cementitious composites developed using a novel dispersion technique, *Cement Concr. Res.* 2015; 73: 215–227. <https://doi.org/10.1016/j.cemconres.2015.03.006>
38. Nochaiya T., Chaipanich A. Behavior of multi-walled carbon nanotubes on the porosity and microstructure of cement-based materials, *Appl. Surf. Sci.* 2011; 257. <https://doi.org/10.1016/j.apusc.2010.09.030>, 1941–5
39. Najjar M.F., Soliman A.M., Nehdi M.L. Critical overview of two-stage concrete: properties and applications, *Construct. Build. Mater.* 2014; 62: 47–58. <https://doi.org/10.1016/j.conbuildmat.2014.03.021>
40. Irshidat M.R., Al-Shannaq A. Using textile reinforced mortar modified with carbon nano tubes to improve flexural performance of RC beams, *Compos. Struct.* 2018; 200: 127–134. <https://doi.org/10.1016/j.compstruct.2018.05.088>
41. Vairagade V.S., Dhale S.A. Impact resistance of hybrid steel fiber reinforced concrete, *Hybrid Advances* 2023; 3: 100048. <https://doi.org/10.1016/j.hybadv.2023.100048>
42. Murali G., Vinodha E. Experimental and analytical study of impact failure strength of steel hybrid fibre reinforced concrete subjected to freezing and thawing cycles, *Arabian J. Sci. Eng.* 2018; 43: 5487–5497. <https://doi.org/10.1007/s13369-018-3202-6>
43. Mohammed B.S., Haruna S., Wahab M.M.A., Liew M.S., Haruna A. Mechanical and microstructural properties of high calcium fly ash one-part geopolymer cement made with granular activator, *Heliyon* 2019; 5. <https://doi.org/10.1016/j.heliyon.2019.e02255>
44. Ikraiam F.A., El-latif A.A., Elazziz A.A., Ali J.M. Effect of steel fiber addition on mechanical properties and γ -ray attenuation for ordinary concrete used in El- Gabal El-Akhdar area in Libya for radiation shielding purposes, *Arab J Nucl Sci Appl* 2009; 42: 287–295.
45. Li J.J., Niu J.G., Wan C.J., Jin B., Yin Y.L. Investigation on mechanical properties and microstructure of high performance polypropylene fiber reinforced lightweight aggregate concrete, *Construct. Build. Mater.* 2016; 118: 27–35. <https://doi.org/10.1016/j.conbuildmat.2016.04.116>
46. Han J., Liu Z., Zhang C. Experimental study on impact resistance of steel-fiber-reinforced two-grade aggregate concrete, *Construct. Build. Mater.* 2023; 373. <https://doi.org/10.1016/j.conbuildmat.2023.130901>
47. Mohammed A.A., Karim S.H. Impact strength and mechanical properties of high strength concrete containing PET waste fiber, *J. Build. Eng.* 2023; 68. <https://doi.org/10.1016/j.jobe.2023.106195>
48. Yusuf M.O., Megat Johari M.A., Ahmad Z.A., Maslehuddin M. Evolution of alkaline activated ground blast furnace slag-ultrafine palm oil fuel ash based concrete, *Mater. Des.* 2014; 55: 387–393. <https://doi.org/10.1016/j.matdes.2013.09.047>
49. Ibrahim M., Megat Johari M.A., Rahman M.K., Maslehuddin M. Effect of alkaline activators and binder content on the properties of natural pozzolan-based alkali activated concrete, *Construct. Build. Mater.* 2017; 147: 648–660. <https://doi.org/10.1016/j.conbuildmat.2017.04.163>
50. Fantilli A.P., Chiaia B., Gorino A. Fiber volume fraction and ductility index of concrete beams, *Cement Concr. Compos.* 2016; 65: 139–149. <https://doi.org/10.1016/j.cemconcomp.2015.10.019>
51. Yahaghi J., Muda Z.C., Beddu S.B. Impact resistance of oil palm shells concrete reinforced with

- polypropylene fibre, *Construct. Build. Mater.* 2016; 123: 394–403. <https://doi.org/10.1016/j.conbuildmat.2016.07.026>
52. Murali G., Ramprasada K. A feasibility of enhancing the impact strength of novel layered two stage fibrous concrete slabs, *Eng. Struct.* 2018; 175. <https://doi.org/10.1016/j.engstruct.2018.08.034>
 53. Silvestro L., Jean Paul Gleize P. Effect of carbon nanotubes on compressive, flexural and tensile strengths of Portland cement-based materials: a systematic literature review, *Construct. Build. Mater.* 2020; 264. <https://doi.org/10.1016/j.conbuildmat.2020.120237>
 54. Wang Z., Yan J., Lin Y., Fan F., Sun M. Experimental and analytical study on the double steel plates-UHPC sandwich slabs under low-velocity impact, *Thin-Walled Struct.* 2023; 184. <https://doi.org/10.1016/j.tws.2023.110548>
 55. Rithanyaa R., Murali G., Salaimanimagudam M.P., Fediuk R., Abdelgader H.S., Siva A. Impact response of novel layered two stage fibrous composite slabs with different support type, *Structures* 29 2021; 1–13. <https://doi.org/10.1016/j.istruc.2020.11.004>
 56. Chen C., Zhang X., Hao H. Investigation on the impact resistance of reinforced geopolymer concrete slab, *J. Clean. Prod.* 2023; 406. <https://doi.org/10.1016/j.jclepro.2023.137144>
 57. Yu R., Spiesz P., Brouwers H.J.H. Static properties and impact resistance of a green ultra-high performance hybrid fibre reinforced concrete (UHPRC): experiments and modeling, *Construct. Build. Mater.* 2014; 68: 158–171. <https://doi.org/10.1016/j.conbuildmat.2014.06.033>
 58. Asrani N.P., Murali G., Parthiban K., Surya K., Prakash A., Rathika K., et al. A feasibility of enhancing the impact resistance of hybrid fibrous geopolymer composites: experiments and modelling, *Construct. Build. Mater.* 2019; 203: 56–68. <https://doi.org/10.1016/j.conbuildmat.2019.01.072>
 59. Süper W. Rechnerische Untersuchung Starting Beanspruchen Stahlbetonplatten, *Forsch. Kolloquium Dortmund, Lehrstuhl für Beton-Und Stahlbetonbau*, n.d, 1980.
 60. Murali G., Venkatesh J., Lokesh N., Nava T.R., Karthikeyan K. Comparative experimental and analytical modeling of impact energy dissipation of ultra-high performance fibre reinforced concrete, *KSCE J. Civ. Eng.* 2018; 22. <https://doi.org/10.1007/s12205-017-1678-3>
 61. Abirami T., Loganaganandan M., Murali G., Fediuk R., Vickhram Sreekrishna R., Vignesh T., et al. Experimental research on impact response of novel steel fibrous concretes under falling mass impact, *Construct. Build. Mater.* 2019; 222. <https://doi.org/10.1016/j.conbuildmat.2019.06.175>
 62. Karthikeyan M., Verapathran M., Abid S.R., Murali G. The combined effect of glass fiber mesh and steel fiber on two-layered preplaced aggregate concrete against drop weight impact, *Materials* 2022; 15. <https://doi.org/10.3390/ma15165648>
 63. Zhao J., Xie J., Wu J., Zhao C., Zhang B. Workability, compressive strength, and microstructures of one-part rubberized geopolymer mortar, *J. Build. Eng.* 2023; 68. <https://doi.org/10.1016/j.jobe.2023.106088>
 64. Dong S., Wang D., Ashour A., Han B., Ou J. Nickel plated carbon nanotubes reinforcing concrete composites: from nano/micro structures to macro mechanical properties, *Compos. Appl. Sci. Manuf.* 2021; 141. <https://doi.org/10.1016/j.compositesa.2020.106228>
 65. Carriço A., Bogas J.A., Hawreen A., Guedes M. Durability of multi-walled carbon nanotube reinforced concrete, *Construct. Build. Mater.* 2018; 164: 121–133. <https://doi.org/10.1016/j.conbuildmat.2017.12.221>
 66. Murali G., Karthikeyan K., Senthilpandian M., Wong L.S., Abid S.R., Kumar A.H. Synergistic effects of graphene oxide, steel wire mesh and fibers on the impact resistance of preplaced aggregate concrete. *Journal of Building Engineering.* 2024 Oct 15; 95: 110363. <https://doi.org/10.1016/j.jobe.2024.110363>
 67. Implementing Building Information Modeling in Architectural, Engineering and Construction Education: A Systematic Literature Review; <https://doi.org/10.47857/irjms.2024.v05i04.01718>
 68. An Overview about Using the 3D Printing Technology; <https://doi.org/10.47857/irjms.2022.v03i01.064>
 69. Van Cao V. Performance of NSM GFRP Retrofitted Postfire RC Slabs Under Monotonic and Cyclic Loadings. *Civil Engineering Journal.* 2024 Jun 1; 10(6): 1987–2006. <https://doi.org/10.28991/CEJ-2024-010-06-017>
 70. Sorilla J., Chu T.S., Chua A.Y. A UAV based concrete crack detection and segmentation using 2-stage convolutional network with transfer learning. *HighTech and Innovation Journal.* 2024 Sep 1; 5(3): 690–702. <https://doi.org/10.28991/HIJ-2024-05-03-010>
 71. Elbially S., Elfarnsawy M., Salah M., Abdel-Aziz A., Ibrahim W. An Experimental study on steel fiber effects in high-strength concrete slabs. *Civil Engineering Journal.* 2025 Jan 1; 11(1): 215–29. <https://doi.org/10.28991/CEJ-2025-011-01-013>